Controlling formations of multiple mobile robots*

Jaydev P. Desai Jim Ostrowski Vijay Kumar

General Robotics and Active Sensory Perception (GRASP) Laboratory, University of Pennsylvania
3401 Walnut Street, Room 301C, Philadelphia, PA 19104-6228

Abstract

In this paper we investigate feedback laws used to control multiple robots moving together in a formation. We propose a method for controlling formations that uses only local sensor-based information, in a leader-follower motion. We use methods of feedback linearization to exponentially stabilize the relative distance and orientation of the follower, and show that the zero dynamics of the system are also (asymptotically) stable. We demonstrate in simulation the use of these algorithms to control six robots moving around an obstacle. These types of control laws can be used to control arbitrarily large numbers of robots moving in very general types of formations.

Keywords: Nonholonomic motion planning, Control theory and Formations of robots.

1 Introduction

This paper addresses issues of control and coordination for many robots moving in formation using decentralized controllers. The research on control and motion planning for mobile robots is both extensive and diverse. In the area of mobile robots, optimal motion plans for a single car-like robot have been thoroughly studied, including results of Reeds and Shepp [1], who proved that optimal paths in a free environment consist of straight lines and circular arcs. Other researchers [2] have studied the development of motion plans for mobile robots in the presence of obstacles, and in particular for systems using only local, or sensor-based, planning. One avenue of past research that we have pursued is to use variational methods to obtain optimal motion plans in the presence of obstacles by considering the dynamics of the mobile manipulators [3]. However, the search for optimal motion plans can be computationally very expensive, particularly as the number of robots or degrees of freedom of the system gets large. For this reason, we pursue in the current work easily computable feedback laws that can be used in conjunction with a higher level (but lower complexity) motion planner.

*This material is based upon work supported by the U.S. Army Research Office under grant DAAH04-96-1-0007, the Defense Advanced Research Projects Agency under grant N00014-92-J-1647, and the National Science Foundation under grants BES92-16691, BES92-21796 and CMS91-57156. The first author is also supported by a Fellowship (NSF grant SHR89-20230) from the Institute for Research in Cognitive Science at the University of Pennsylvania.

In the area of nonholonomic systems (which includes most wheeled mobile robots), a great deal of research has been done, particularly in the area of nonlinear control. For example, several researchers have studied planning algorithms for mobile robots, with more recent efforts focused on using time-varying [4] and non-smooth feedback laws to generate exponentially stabilizing controllers [5]. In our current study, we show that for a restricted class of tracking motions (line segments and circular arcs), the smooth state feedback laws developed here also provide asymptotic convergence to a nominal steady-state trajectory.

On the other hand, many researchers have recently investigated controlling multiple (i.e., many) cooperative robots [6, 7]. This research has primarily focused on generating emergent or complex behaviors from organizations of many small, individual, and often heterogeneous robots. Generally, these approaches either require some type of supervisory (centralized) control and process planning, or rely on more evolutionary approaches to generate a pre-specified system behavior. The goal we pursue here is different than these approaches in that we target a specific goal and attempt to generate rigorously provable measures/bounds on the performance of our system.

We formulate the problem of control and coordination for many robots moving in formation using decentralized controllers as one in which a motion plan for the overall formation is given, for example, using methods from optimal control or some other external source such as human operator. This motion plan is then used to control a single lead robot. We assume that each robot has the ability to measure the relative position of other robots that are immediately adjacent to it. Once the motion for the lead robot is given, the remainder of the formation is governed by local control laws based on the relative dynamics of each of the follower robots and the relative positions of the robots in the formation. These control laws have the advantage of providing easily computable, real-time feedback control, with provable performance for the entire system.

In this paper we describe two scenarios for feedback control within a formation. In the first scenario, one robot follows another by controlling the relative distance and orientation between the two. This situation is applicable to all formations in which each robot has one leader except for the lead robot. Thus it can be used for robots marching in a single file. In the second scenario, a robot maintains its position in the formation by maintaining a specified distance

from two robots, or from one robot and an obstacle in the environment. This behavior is useful for robots that are constrained by more than one robot (or obstacle) in the formation. This is true, for example, for robots that are internal to (or inside) a formation of robots marching in a rectangular formation with a rows and b columns, or for a robot in a single file formation marching very near an obstacle where the robot must maintain a specified separation from the leader as well as a specified separation from the obstacle. We demonstrate the use of these techniques in several simulations, including motions in formation with up to six robots and obstacles. Extensions to many more robots is quite straightforward, and not computationally burdensome.

In Section 2, we discuss two types of feedback control laws for maintaining the formation. We then present several numerical simulations to illustrate the procedure in Section 3 and finally make some concluding remarks in Section 4.

2 Control of formations

We assume that the motion of the lead robot is planned, and focus our attention on controlling the internal geometries of the formation. For our purposes, we use tools from optimal control theory developed in [3] to specify the motion of the lead robot which can be computed by minimizing a suitable cost function. Thus the trajectory and velocity computed by the method of [3] is transmitted to the first generation of robots in the chain which act as leaders for the other follower robots in the formation.

2.1 Feedback control

In this section we develop two types of feedback controllers for maintaining formations of multiple mobile robots.

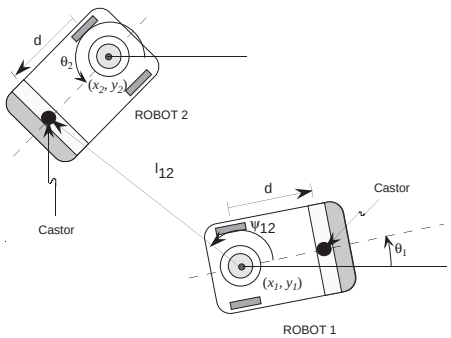

Figure 1: Notation for $l-\psi$ control

$\mathbf{l-\psi}$ control: In Fig. 1, we show a system of two nonholonomic mobile robots separated by a distance of l_{12} between the center of the first robot and the front castor of the second robot. The distance between the castor and the center of the axis of the wheels of each robot is denoted by d. Each robot has two actuated degrees-of-freedom. The two robots are not physically coupled in any way and the aim of the feedback controller is to maintain the desired formation. The state of the system is given by: $[l_{12}, \psi, \theta]^T$

In the $l-\psi$ control of the two mobile robots, the aim is to maintain a desired length, l_{12}^d and a desired relative angle ψ_{12}^d between the two robots. The kinematic equations for the system of two mobile robots shown in Fig. 1 is given by:

$$\begin{aligned} \dot{x}_i &= v_i \cos\theta_i \\ \dot{y}_i &= v_i \sin\theta_i \\ \dot{\theta}_i &= \omega_i \end{aligned} \tag{1}$$

for the first robot and:

$$\begin{aligned} \dot{l}_{12} &= v_2 \cos\gamma_1 - v_1 \cos\psi_{12} + d\omega_2 \sin\gamma_1 \\ \dot{\psi}_{12} &= \frac{1}{l_{12}}\{v_1 \sin\psi_{12} - v_2 \sin\gamma_1 + d\omega_2 \cos\gamma_1 - l_{12}\omega_1\} \\ \dot{\theta}_2 &= \omega_2 \end{aligned} \tag{2}$$

for the second robot where, $\gamma_1 = \theta_1 + \psi_{12} - \theta_2$ and v_i, ω_i $(i = 1, 2)$, are the linear and angular velocities at the center of the axle of each robot. In order to avoid collisions between robots, we will require that $l_{12} > d$.

We use standard techniques of I/O linearization [8] to generate a control law that gives exponentially convergent solutions in the internal shape variables l_{12} and ψ_{12}. The control law is given by:

$$\begin{aligned} \omega_2 = \frac{\cos\gamma_1}{d}\{&\alpha_2 l_{12}(\psi_{12}^d - \psi_{12}) - v_1 \sin\psi_{12} + l_{12}\omega_1 + \\ &\rho_{12}\sin\gamma_1\} \\ v_2 = \rho_{12} - d\omega_2 \tan\gamma_1 \end{aligned} \tag{3}$$

where

$$\rho_{12} = \frac{\alpha_1(l_{12}^d - l_{12}) + v_1 \cos\psi_{12}}{\cos\gamma_1}.$$

This leads to dynamics in the $l-\psi$ variables of the form:

$$\begin{aligned} \dot{l}_{12} &= \alpha_1(l_{12}^d - l_{12}) \\ \dot{\psi}_{12} &= \alpha_2(\psi_{12}^d - \psi_{12}). \end{aligned}$$

Proposition 1 *Assume the system of two mobile robots shown in Fig. 1 and the associated control law in (3). For the motion of the lead robot following a circular path, $v_1 = K_1$, $\omega_1 = K_2$, θ_2 is locally asymptotically convergent to $\theta_1(t) + \psi_{12}^d - \beta_2 - \arccos(K_2/\beta_1)$, where* $\beta_1 = \sqrt{\left(\frac{K_2 l_{12} + K_1 \sin\psi_{12}^d}{d}\right)^2 + \left(\frac{K_1 \cos\psi_{12}^d}{d}\right)^2}$, $\beta_2 = \arctan\left(\frac{K_1 \cos\psi_{12}^d}{K_2 l_{12} + K_1 \sin\psi_{12}^d}\right)$.

Proof: Since l_{12} and ψ_{12} are exponentially stabilized, we focus our attention on the zero dynamics of the system, which for this case is given in terms of θ_2. We seek to show that the zero dynamics of the system are asymptotically stable, i.e., the system is *asymptotically minimum phase* [8].

The differential equation for θ_2 is given by:

$$\dot{\theta}_2 = \frac{K_2 l_{12} + K_1 \sin\psi_{12}^d}{d}\cos(K_2 t - \theta_2 + \theta_{10} + \psi_{12}^d) + \frac{K_1 \cos\psi_{12}^d}{d}\sin(K_2 t - \theta_2 + \theta_{10} + \psi_{12}^d)$$

The above equation can be re-written as:

$$\dot{\theta}_2 = \beta_1 \cos(K_2 t - \theta_2 + \theta_{10} + \psi_{12}^d - \beta_2)$$

where β_1 and β_2 are as given in the proposition.

We make a change of variables to $\delta_{12} = \theta_1 - \theta_2 = K_2 t + \theta_{10} - \theta_2$, which gives the following differential equation:

$$\dot{\delta}_{12} = K_2 - \beta_1 \cos(\delta_{12} + \psi_{12}^d - \beta_2). \qquad (4)$$

The equilibrium point, $\delta_{12}^e = -\psi_{12}^d + \beta_2 + \arccos(K_2/\beta_1)$, is easily shown to be asymptotically stable, using a linearization of (4). Thus, the motion of the robots will locally converge to the equilibrium trajectory, $\theta_2^e = \theta_1 - \delta_{12}^e = \theta_1(t) + \psi_{12}^d - \beta_2 - \arccos(K_2/\beta_1)$.

□

Corollary 2 *For the case that the lead robot follows a straight line ($\omega_1 = K_2 = 0$), θ_2 converges exponentially to θ_{10}.*

Proof: For $v_1 = K_1$ and $\omega_1 = 0$, we obtain the following expression for ω_2 after some algebraic manipulations:

$$\omega_2 = \dot{\theta}_2 = \frac{K_1}{d}\sin(\theta_{10} - \theta_2) \qquad (5)$$

where, θ_{10} is the initial orientation of the first robot at the beginning of the motion (and maintained as a constant throughout the motion since $\omega_1 = 0 \Rightarrow \theta_1(t) = \theta_{10}$). Integrating the expression and assuming $\theta_2(0) = \theta_{20}$, we get:

$$\tan\left(\frac{\theta_2 - \theta_{10}}{2}\right) = \tan\left(\frac{\theta_{20} - \theta_{10}}{2}\right)\exp^{-\frac{K_1}{d}t}$$

As $t \to \infty$, $\theta_2 \to \theta_{10}$ and θ_2 exponentially converges to θ_{10}. □

Remarks:

1. Note that we can solve explicitly for the motion of θ_2 as

$$\frac{\tan\frac{\delta_{12}+\psi_{12}^d-\beta_2}{2} + \sqrt{\frac{\beta_1-K_2}{\beta_1+K_2}}}{\tan\frac{\delta_{12}+\psi_{12}^d-\beta_2}{2} - \sqrt{\frac{\beta_1-K_2}{\beta_1+K_2}}} = C_0 \exp^{-\sqrt{\beta_1^2-K_2^2}\,t}$$

where $\delta_{12} = K_2 t + \theta_{10} - \theta_2$, β_1 and β_2 are as defined in the proposition and $\beta_1^2 > K_2^2$ (since $l_{12} > d$). C_0 is the constant of integration.

2. Based on the results of Proposition 1, it is clear that there is a constant offset, $\delta_{12}^e = \theta_1 - \theta_2$, in steady state. If we assume that the lead robot is moving in a straight line, then we arrive at the result of Corollary 2.

3. The optimal point-to-point paths of a nonholonomic car with constraints on the turning radius were shown by Reeds and Shepp [1] to be composed of straight lines and circular arcs. This is seen to be generally true even for more complicated systems from the numerical results presented in [9]. Hence, in this section, we only investigate motions involving straight lines and circular arcs.

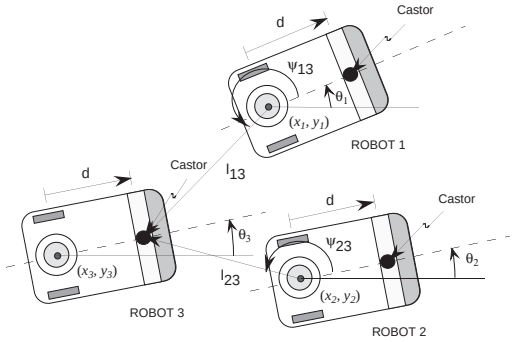

Figure 2: Notation for $l-l$ control

$\mathbf{l-l}$ control: In Fig. 2, we show a system of three nonholonomic mobile robots. The task involves stabilizing the distance of the third robot from the other two robots. Thus the state of the third robot is specified by $(l_{13}, l_{23}, \theta_3)^T$. Distances are measured from the center of the axle of the first two robots to the castor of the third robot which is offset by d from its axle. Each robot has two actuated degrees-of-freedom. The three robots are not physically coupled in any way and the aim of the feedback controller is to maintain the desired formation.

In the $l-l$ control, the aim is to maintain the desired lengths, l_{13}^d and l_{23}^d of the third robot from its two leaders. Again, we assume that both l_{13} and $l_{23} > d$. Additionally, we require that the follower robot never lies on the line connecting the two lead robots. In particular, this requires that the two lead robots never separate by a distance greater than $l_{13}^d + l_{23}^d$.

The kinematic equations for the system of three mobile robots shown in Fig. 2 is given by (1) for $i = 1, 2$ and

$$\begin{aligned} \dot{l}_{13} &= v_3\cos\gamma_1 - v_1\cos\psi_{13} + d\omega_3\sin\gamma_1 \\ \dot{l}_{23} &= v_3\cos\gamma_2 - v_2\cos\psi_{23} + d\omega_3\sin\gamma_2 \\ \dot{\theta}_3 &= \omega_3 \end{aligned} \qquad (6)$$

for the third robot where, $\gamma_i = \theta_i + \psi_{i3} - \theta_3$ $(i = 1, 2)$.

Again, we use I/O linearization to generate a feedback control law:

$$\omega_3 = \frac{1}{d\sin(\gamma_1 - \gamma_2)}\left\{\alpha_1(l_{13}^d - l_{13})\cos\gamma_2 + v_1\cos\psi_{13}\cos\gamma_2 - \alpha_2(l_{23}^d - l_{23})\cos\gamma_1 - v_2\cos\psi_{23}\cos\gamma_1\right\}$$

$$v_3 = \frac{\alpha_1(l_{13}^d - l_{13}) + v_1\cos\psi_{13} - d\omega_3\sin\gamma_1}{\cos\gamma_1}. \qquad (7)$$

This gives exponential convergence for the controlled variables:

$$\begin{aligned} \dot{l}_{13} &= \alpha_1(l_{13}^d - l_{13}) \\ \dot{l}_{23} &= \alpha_2(l_{23}^d - l_{23}). \end{aligned} \tag{8}$$

Proposition 3 *Assume a system of three mobile robots as in Fig. 2 and the associated control law given by (7). For a straight line parallel motion of the first two robots (constant velocity $v_1 = v_2 = K$, $\omega_1 = \omega_2 = 0$ and $\theta_{10} = \theta_{20} = \theta_0$), θ_3 locally converges exponentially to $\theta_3^e = \theta_0$ and $\psi_{13}(t) = \psi_{13}(0)$ and $\psi_{23}(t) = \psi_{23}(0)$.*

Proof: The proofs are similar in nature to those presented for $l - \psi$ feedback control. Restricting our attention to the zero dynamics, the above $l - l$ control law gives

$$\begin{aligned} \dot{\theta}_3 &= \frac{K}{d}\sin(\theta_0 - \theta_3) \\ \dot{\psi}_{13} &= 0 \\ \dot{\psi}_{23} &= 0 \end{aligned} \tag{9}$$

Integrating the expression and assuming $\theta_3(0) = \theta_{30}$, we get:

$$\tan\left(\frac{\theta_3 - \theta_0}{2}\right) = \tan\left(\frac{\theta_{30} - \theta_0}{2}\right)\exp^{-\frac{K}{d}t}.$$

As $t \rightarrow \infty$, $\theta_3 \rightarrow \theta_0$ and θ_3 exponentially converges to θ_0. Hence, the solution $\theta_3^e = \theta_0$ is a stable equilibrium point. Similarly the other two differential equations for ψ_{13} and ψ_{23} gives constant value for all time, t, namely, $\psi_{13}(0)$ and $\psi_{23}(0)$ respectively. □

Thus, the choice of configuration variables is dependent on the type of control law employed to control the motion of a robot. For example in the case of $l - \psi$ control, the configuration variables of the controlled robot are given by $(l_{ik}, \psi_{ik}, \theta_k)$ and in the case of $l - l$ control, it is given by $(l_{ik}, l_{jk}, \theta_k)$, where i, j refers to the subscript for the lead robot/robots and k refers to the subscript for the controlled robot. For a long chain of robots moving with a particular formation, the first robot in the chain plans an optimal path, avoiding any obstacles. Its velocity and trajectory information is then conveyed to the first generation of robots in the chain and they in turn act as the lead robots for subsequent generations down the chain.

2.2 Graphs of formations

We can think of a formation as being made up of two components: a) a directed relational graph structure, or *diagraph*, that represents the internal topology of the formation, and b) the *shape variables* that describe its internal state. Graphs in this paper are "directed graphs" or *diagraphs* [10], as the lead robot is used to control the other follower robots in the formation. The arrows are thus directed from the lead robot to the follower robot in the formation. In this context, specific formations lead to the development of unique diagraphs, and a particular set of shape variables associated with each graph structure. The types of control investigated here, such as the $l - \psi$ control law, lead us naturally to the study of *trees*. A *tree* is a connected acyclic graph. Sometimes in the presence of obstacles it is necessary to switch from one diagraph to another and this leads to internal dynamics of graphs and hence the resulting graph is non-isomorphic to the original graph. Two graphs, G and H are said to be *isomorphic* if there exists a one-to-one correspondence between their point sets which preserve adjacency. Consider for example the two graphs, G and H shown in the figure below. The graph H is the desired graph when there is a very narrow constriction and hence the robots must change to a single file formation. In that situation the original graph, G needs to transform to H and hence the various controller interdependencies must also change. Shown in the same figure is another formation, J, which is isomorphic to G. The change in the formations should be such that the subsequent generations of robots can obtain sensory data from the robot immediately ahead of them and hence can autonomously carry out their motions. One of the possible avenues of future research is to study the transitions from one graph to another which are non-isomorphic in order to overcome obstacles in the environment. In the following section, we investigate the changes in formation between isomorphic graphs and demonstrate when the controller interdependencies change in the presence of obstacles.

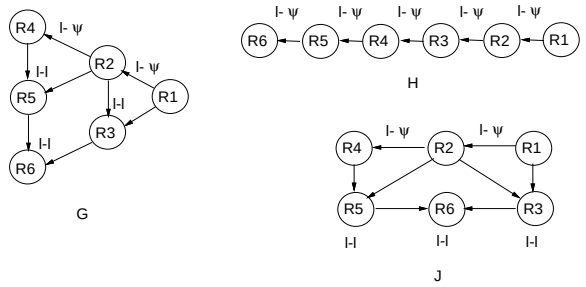

Figure 3: Isomorphic and Non-isomorphic diagraphs

Once a specific graph has been chosen to represent a formation, the shape variables can be associated to the graph, and the dynamics governing them written down as in Eqs. 2 and 6. In choosing the two pairings of variables for the internal dynamics, we have attempted to formulate the problem in a manner similar to previous work on geometric formulations of locomotion systems [11]. In the geometric setting, one can use the natural symmetries of the problem to decouple the study of locomotion into two basic constituents: motion of the body as a whole, generally associated to motion within a Lie group, G, and motion of the internal shape of the body, described by some shape manifold, M. In this setting, the effect of shape changes on locomotion can be written succinctly as

$$g^{-1}\dot{g} = -A(r)\dot{r} \tag{10}$$

$$\dot{r} = u, \tag{11}$$

where $g \in G$, $r \in M$, and u represents the control inputs, and the map A is called a *connection*.

We have attempted to use similar techniques in this paper, where one can think of changes in formation as changes in the internal shape of the body (or alternatively, as changes in the graph). One can then draw the analogy with biological systems, for example, paramecia or snakes, which can deform their internal shape in order to move through narrow passageways. This would parallel our use of changes in formation (discussed below) from a triangular formation to a march-abreast formation in order to move through a narrow corridor. For the present case, the internal symmetries of the problem are reflected in the position and orientation of the invariance of the lead robot[1]. This allows us to write the shape dynamics in a form similar to (11) above, in which the group variables have effectively been removed from the equations. This is a point that requires further study, in order to utilize fully the geometry of these types of systems.

3 Results

Next, we show the implementation of these control laws in simulation using several examples.

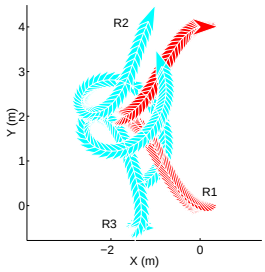

Figure 4: Parallel parking

Moving in constant formation: We first consider an example of parallel parking without any obstacles in the environment. The lead robot denoted $R1$ plans an optimal path as shown in Fig. 4. In this example we only show two follower robots and they are both controlled by an $l-\psi$ control law. Using the notation of Fig. 1, the configuration of the system of three robots is given by $[x_1, y_1, \theta_1, l_{12}, \psi_{12}, \theta_2, l_{13}, \psi_{13}, \theta_3]^T$. In this example, the lead robot's ($R1$) optimal path minimizes the distance traveled in the parallel displacement of $4m$ and its path is as shown in Fig. 4. Also shown is the snapshot at various instants of time of the three robots moving in formation.

In the second example, we demonstrate the case of 6 robots moving around an obstacle. The initial formation of these robots with their controller interdependencies is as shown in Fig. 5. In both the examples shown in Fig. 6 and Fig. 7, we demonstrate the switching that occurs in the controllers in the presence of obstacles. In Fig. 6, $R1$ executes a straight

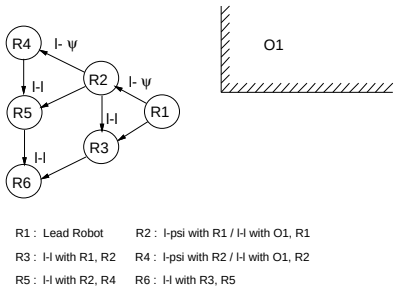

Figure 5: Controller schematic

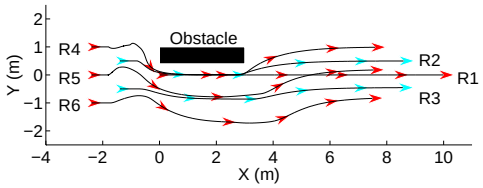

Figure 6: Obstacle : Example 1

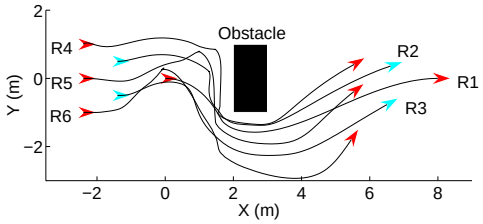

Figure 7: Obstacle : Example 2

line path from $(0,0,0)$ to $(10,0,0)$. As proved in Section 2.1, we would expect the orientations of the followers to exponentially stabilize to that of the lead robot, R_1, after they overcome the obstacle. This is observed in the plot shown in Fig. 6. Initially when the lead robot follows the straight line, the follower robots, R_2 and R_4 are controlled by the $l-\psi$ feedback law while the other robots are controlled by the $l-l$ feedback law as shown in Fig. 5. However, when R_2 and R_4 move within a predefined distance of the obstacle, they switch from the $l-\psi$ controller to an $l-l$ controller, where one of the distances is the distance to the obstacle. This guarantees that the robots are a predefined distance away from the obstacle. After the obstacle is overcome and the distance of R_2 and R_4 exceeds the threshold, it switches back to the $l-\psi$ controller. This is observed in the paths shown in Fig. 6.

In Fig. 7, the optimal path for $R1$ is computed by minimizing a suitable norm which could be the norm of velocities or the actuator forces. The initial and final configuration of $R1$ is from $(0,0,0)$ to $(8,0,0)$. The trajectories for all the robots are as shown in Fig. 7. The transition in the controller interdependencies is

[1] Actually, the invariance in orientation requires that all orientation variables, θ_i, be shifted by the same amount.

very similar to that illustrated in Fig. 6. Although it is difficult to see this from the figure, all of the robots move without contacting each other (or the obstacle).

Change in formation : Finally, we very briefly describe the use of these methodologies to change formation. In this section we illustrate with an example the change in formation of a formation of robots as might be done in order to squeeze through a constriction. Shown in Fig. 8 is a formation of six robots arranged in the triangular formation and the task is to change the formation from a triangular one to a rectangular one. Shown in the same figure is the initial and final configuration of these robots and the paths of each of them. We note that there is no collision among the robots during this transition phase from the triangular formation to the rectangular one. This is a formation change that is performed by changing only the shape variables and not the graph of the formation.

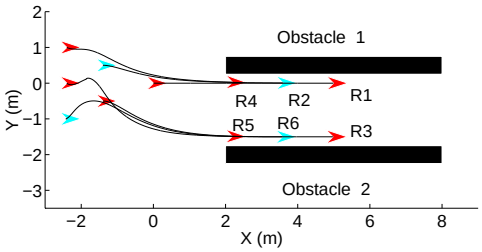

Figure 8: Change in formation

4 Conclusions

In this paper we have studied strategies for controlling formations of mobile robots using methods from nonlinear control theory. For the current work, we have focused on decomposing the problem of controlling formations into one of controlling a single robot's motion in following one or two lead robots. We use the terms $l-\psi$ and $l-l$ control to reflect whether the control laws are based on tracking the position and orientation of the robot relative to a lead robot, or the position relative to two lead robots, respectively. It is assumed that there is a single lead robot for the overall formation whose motion plans are generated externally. The results presented in this paper apply to general formations moving through an environment that may include obstacles. The two controllers proposed here are used to achieve this objective. The $l-\psi$ and the $l-l$ controller guarantee the correct formation, while the modified $l-l$ controller can also be used to change the shape of our formation in the presence of obstacles.

We contrast this approach to our former work using optimal control methods [3, 9]. These tools provide excellent open loop plans, but tend to incur much higher computational costs as the number of robots in the formation increases. For this reason, we use these methods to plan an optimal collision free path for the lead robot and use that information to control the fleet of follower robots. This method lends itself to a great advantage for on-line motion planning. The computation time typically for three robots avoiding a circular obstacle requires at least 2 min. for a specifically tailored compiled code and the formation may also not be necessarily maintained. In contrast, the motion for the formation of six robots around an obstacle of higher complexity or the one shown in Fig. 7 has a run time of about 5 s. in Matlab.

We also envision that the results from graph theory and the geometric techniques related to robotic locomotion will ultimately enable us to construct explicit maps going from one formation to another. In other words, we would like to have the ability to generate smooth transitions between non-isomorphic graphs. This might be particularly useful in moving through narrow passageways, or past other obstructions in the environment. The use of shape changes to effect these types of transitions will play a key role in these types of transformations. Another critical issue is the propagation of the effects of sudden changes in the motion of the lead robot in the presence of uncertainities through the formation. These topics are the subject of our future work in this area.

References

[1] J. A. Reeds and L. A. Shepp, "Optimal paths for a car that goes both forwards and backwards," *Pacific. Journal of Math.*, vol. 145, no. 2, pp. 367–393, 1990.

[2] L. Kavraki, P. Švestka, J. C. Latombe, and M. H. Overmars, "Probabilistic roadmaps for path planning in high-dimensional configuration space.," *IEEE Transactions on Robotics and Automation*, vol. 12, no. 4, pp. 566–580, 1996.

[3] J. P. Desai and V. Kumar, "Nonholonomic motion planning for multiple mobile manipulators," in *Proc. of 1997 IEEE Int. Conf. on Robotics and Automation*, (Albuquerque, NM), April 1997.

[4] C. Samson, "Time-varying feedback stabilization of car-like wheeled mobile robots," *The International Journal of Robotics Research*, vol. 12, no. 1, pp. 55–64, 1993.

[5] O. Egeland, E. Berglund, and O. J. Sordalen, "Exponential stabilization of a nonholonomic underwater vehicle with constant desired configuration," in *Proc. of 1994 IEEE Int. Conf. on Robotics and Automation*, (San Diego, CA), pp. 20–25, May 1994.

[6] T. Balch and R. Arkin, "Communication in reactive multiagent robotic systems," *Autonomous Robots*, vol. 1(1), pp. 27–52, 1994.

[7] X. Yun, E. Paljug, and R. Bajcsy, "Tracs: An experimental multiagent robotic system," in *DARPA Workshop on Software Tools for Distributed Intelligent Control Systems*, (Pacifica, CA), July 1990. Also available as Tech. Report MS-CIS-90-60, University of Pennsylvania.

[8] H. Asada and J.-J. E. Slotine, *Robot Analysis and Control*. New York: John Wiley & Sons, 1986.

[9] J. Desai, C. C. Wang, M. Žefran, and V. Kumar, "Motion planning for multiple mobile manipulators," in *Proc. of 1996 IEEE Int. Conf. on Robotics and Automation*, (Minneapolis, MN), 1996.

[10] F. Harary, *Graph Theory*. New York: Addison-Wesley Publishing Company, 1972.

[11] J. P. Ostrowski and J. W. Burdick, "The geometric mechanics of undulatory robotic locomotion." To appear in the International Journal of Robotics Research, July 1997.